The Fourth International Conference on Cold Fusion, 1993. (ICCF-4) Lahaina, Maui, Dec. 6-9, 1993: Electric Power Research Institute 3412 Hillview Ave., Palo Alto, CA 94304 vol. 2: p. 1.1. Also, *The Fourth International Conference on Cold Fusion*, 1994, *Transactions of Fusion Technology*, Vol. 26, Num. 4T, Part 2, December 1994, p. 267.

TRIGGERING OF HEAT AND SUB-SURFACE CHANGES IN Pd-D SYSTEMS

J. O'M Bockris, R. Sundaresan, Z. Minevski and D. Letts
Department of Chemistry, Texas A&M University
College Station, Texas 77843

I. INTRODUCTION

More than four years after the first reports of chemically stimulated nuclear reactions, the triggering of heat evolution and the production of associated nuclear debris remains a highly uncertain matter. Both the duration of the switch-on time and, indeed, whether a given electrode will commence to show nuclear activity within 500 hours of the beginning of electrolysis, remain unclear.[1]

In the present study, three methods of triggering anomalous heat are described. The changes in the sub-surface of palladium during the evolution of D_2 or H_2 are described as a function of potential, temperature and time.

Finally, these results are evaluated against the present theories of heat production in metals.

II. EXPERIMENTAL

II.1. Electrochemical Stimulation

Hodko and Bockris (1) presented a pulsing study in the 1991 Meeting in Como. In that study, when an electrode with D (D/Ph form 0.3 to 0.83) was emptied or filled, heat bursts were initiated. The present study examines the efficacy of the Takahashi conditions.

Electrolysis Cell: The cell was made of plexiglass, which was 5 mm thick. It had outer dimensions of 120 mm × 75 mm × 100 mm. The cell's lid was made of the same material, with provisions for introducing the electrodes, cooling coil, etc. The cell housed a glass cooling coil with six spirals through which chilled water circulated at a constant rate of ~5 liters per minute to cool the electrolyte. The chilled water was maintained at 20±0.01°C in an external cooling system (Haake, Model A81). This arrangement ensured an efficient exchange of heat between the electrolyte (source of heat) and the chilled water coils (sink). Thermal equilibrium was reached within 30 or 40 minutes.

Electrodes: A 1 mm thick, 25 mm square plate of palladium metal served as the cathode. This material was received as a gift from Tanaka Kikinzoku Kogyo, Japan, and was similar to the Pd used by Takahashi (2). The material was 99.97% pure Pd. It was used as such without pretreatment, supported by two small polyethylene blocks on either side, and surrounded by an anode of 0.5 mm thick platinum wire (Johnson Matthey, Puratronic Grade) which was wound around the blocks (6 turns with ~5 mm pitch) keeping the anode-cathode distance at ~10 mm at both sides. The platinum contact wire to the cathode and the platinum anode lead wire were both covered with Teflon tape to ensure electrical isolation. The electrolyte was 0.29 M LiOD, obtained by dissolving lithium metal (Johnson Matthey, USA, 99.9% pure) in D_2O (ISOTEC. Inc., USA, 99.9 atom percent pure) in an atmosphere of argon. The cell assembly is shown elsewhere (3).

Power Supply: A constant current assembly was used.

Electrolysis Conditions: The cell was filled with 650 ml of electrolyte. The level was kept at 1 cm below the top of the cell. A thermometer was placed near the cooling coil and a thermistor (matched earlier with the thermometer) in between the electrode assembly and the cooling coil. A thermistor thermometer (Omega, USA), with both analog and digital readout was used to record the temperature of the electrolyte during the experiment. The electrolyte level was maintained to within 1 cm of the initial level by replenishing periodically with D_2O. A 1 ml sample was withdrawn every 2 or 3 days to check for tritium. The temperature in the laboratory remained at

20±l°C, except for a period of about 10 days when there was a breakdown in the temperature control and measurements were not taken.

The experimental procedure involved a 'preloading phase' employing a saw-tooth current mode. The current was cycled linearly from 0.25 A to 4.2 A (0.02 - 0.336 $A.cm^{-2}$) in a 20 minute period. This was continued for 9 days. After this, the measurement phase was carried out in the Low - High [L-H] current mode, in which the current was kept constant at 0.25 A and 4.2 A alternately for 6 hour periods. The experiment was carried out over a 61-day duration.

Calibration procedure for excess heat calculation: Calibration by Joule heating was adopted. The experiment was, therefore, started with an initial test operation. Currents of 1A, 3A and 5A were passed through the cell for 40 minutes each and the electrolyte temperature and cell voltages noted. Assuming that there was no excess heat generation at this stage of the experiment, the temperature rise, ΔT, during this period was taken as a measure of the calorimeter calibration. A temperature increase (ΔT) of 4.70°C was recorded for 50W Joule heating. The "zero power" line, corresponding to 20°C, was taken as constant in view of the steady room temperature. A value of 0.094°C was thus obtained for ΔT per watt input power over the experimental range.

Determination of the D/Pd ratio: The degree of loading of deuterium into palladium was monitored 'in situ' by means of four probe resistivity measurements. Four platinum leads were spot-welded to the cathode at appropriate locations and the resistance was continuously recorded by means of a digital micro-ohmmeter (Model DMO-350, Tacrad Inc., Canada) and stored in an IBM-286 compatible computer. The ratio of the initial resistance, R_0, before the electrolysis to the resistance, R, at any time during the experiment was plotted against time. To calculate the value of D/Pd from this plot, use was made of a previously constructed calibration graph of R/R_0 vs. D/Pd (in which the D/Pd determination had been made on the basis of coulometric measurements).

Measurement of the potential of the cathode: A luggin capillary contact tube was placed within 1 mm of the cathode and the cathode potential was measured with respect to a saturated calomel electrode(S.C.E.).

Measurement of tritium: During the experiment, the tritium activity in the electrolyte was monitored every two or three days. A 0.5 ml sample was withdrawn, mixed with 6.5 ml of Optiphase, "HiSafe-3" scintillation cocktail. The activity of this solution was counted for 10 minutes. A Wallac 1410 Liquid Scintillation Counter was used.

II.2. Radio-Frequency Stimulation

Electrolysis cell: A Johnson Matthey palladium foil cathode of 99.9 % purity and dimensions 11.9 mm × 12.5 mm × 1 mm was held between two Teflon holders, and surrounded by 7 turns of 20 gauge platinum wire anode (3) . This electrode assembly was contained in a 10 cm tall cylindrical glass cell of 25.4 mm internal diameter. 15 ml of 0.3 M LiOD in D_2O was taken in the cell for electrolysis.

The temperature was measured by means of a thermistor. The RF power was applied to the cell by means of a 20 gauge copper wire that was wound around the cell in 15 turns in a typical NMR configuration.

RF Generator: A Rohde & Schwarz generator, with a frequency range 100-1000 MHz, was used in conjunction with a RF amplifier (ENI Model 6O3L). The RF power (6 - 100 mW), mentioned in the experiment, is the maximum power delivered assuming 100 % coupling efficiency. The efficiency of the RF-coupling to the cell was not measured.

Measurement of heating due to application of RF power: Prior to the stimulation experiment, different RF power ranging from 100 mW to 1 W were applied to the cell containing the 15 nil electrolyte. The rise in temperature was 5.2° C per Watt.

Before the RF power was coupled to the cell, the palladium cathode was charged with deuterium by carrying out the electrolysis at 0.25 A for 139 hours. The D/Pd ratio was expected to have reached > 0.8 by this procedure. At this stage, maintaining the charging current unchanged, the RF power of 6 to 30 mW was applied to the cell at 365.608 MHz.

II.3. Magnetic Stimulation

The magnetic field was applied by means of two different permanent magnets:

Magnet 1: A horseshoe magnet of 200 Gauss was placed around the cell (3).
Magnet 2: Two 1" diameter disc magnets of Neodymium were placed in attractive mode on opposite sides of the cell; the field strength was measured at the Los Alamos National Laboratory as 800 Gauss in an empty cell (3).

This experiment was carried out at 3.5°C in a small refrigerator. The connecting leads were run through small holes drilled on the sides of the refrigerator which were then sealed with epoxy. The lower temperature was chosen to facilitate deuterium loading.

The cathode was 99.9 % pure Englehardt palladium which had been cold rolled. Its dimensions were 12.5 mm × 12.5 mm × 0.28 mm. It was charged with deuterium at a current of 80 mA (cell voltage was 2.64 V in 15 ml of 0.3 M $LiOD/D_2O$) for 48 hours before applying the magnetic stimulation. It is probable that this treatment corresponded to a D/Pd ratio of > 0.8.

II.4. Materials Science

A standard three electrode electrochemical system was used in this study with Palladium as the working electrode and Platinum as the counter electrode. Working electrodes were in the form of a foil, 50 μm × 10 mm × 5 mm, purchased from Johnson Matthey as 99.975 % pure Palladium. They were used as cathodes in the electrolysis of O.1 M KOH or O.1 M KOD medium with saturated calomel electrode as a reference electrode. Experiments were performed by varying the time of electrolysis and overpotential at room temperature. The potential range studied was from the reversible potential to overpotential of η = - 1.0 V. The applied potentials were maintained for different periods of time, varying from 0.5 hour to 6 weeks.

Each experiment was carried out with a fresh electrode. Following electrolysis at certain conditions, the electrode was washed with purified water and etched in 30 % 1:1 HNO_3 + HC1 mixture. A preliminary investigation had been carried out prior to the experiments to observe the effect of duration of etching on the depth of the surface exposed. Measurements were carried out for durations ranging from 1 to 5 minutes. After etching, the solution was analyzed by ICP. By knowing the area of the etched surface it was calculated that one etching procedure corresponds to the depth of 800 Å per minute. An etching time of 2.5 minutes, corresponding to 2,000 Å was chosen for our investigations. The etched surfaces were then subjected to examination by means of Differential Polarization Interference Contrast Microscopy (DPICM) and Scanning Electron Microscopy (SEM).

DPICM was chosen because it is a technique capable of imaging minute surface structures in differentiating color. At magnifications of 100 and 600 that have been used in this study, it affords greater observability of patterns having dimensions of the order of c. 0.5 mm with a resolution of 2 and 0.4 μm. SEM was chosen because it could image the surface in three dimensions. (It has a large depth of field and shows shadow relief effect of secondary electrons.) At magnifications of 1000 and 50,000, the resolution of 0.2 and 0.004 μm afforded observations of crystal grains.

The microscopy was repeated after re-etching the surface 5 successive times, up to a depth of 1 μm.

III. RESULTS

III.1. Electrochemical Stimulation

The cell voltage during the L-period was almost steady at about 3.6V. The electrolyte temperature was also constant at 20±0.05°C, indicating no excess heat during these periods. During the H-period, there was an appreciable increase in the cell voltage from the initial value of 20V to about 31V towards the conclusion of the

experiment. The corresponding electrolyte temperatures also showed a rise with time.

During the H-period, the fall in the electrolyte level due to electrolysis had an effect on the cell voltage and on the corresponding electrolyte temperature. Therefore, values taken only within a short time (1 or 2 hours) after the initial level was restored by replenishment with D_2O, were taken account of, in calculating excess heat. This seemed reasonable since thermal equilibrium between the cell and the circulating water was always reached within 40 minutes.

If the cell voltage was V and the current I, then the input power for Joule heating, Q_i , would be

$$Q_i = (V - 1.54) * I \tag{1}$$

The output power, Q_{out}, was calculated from the observed rise in the electrolyte temperature, ΔT, by means of the calibration done earlier, i.e.,

$$Q_{out} = \Delta T + (0.094)W \tag{2}$$

The excess power, Q_x., was then arrived at as i.e.,

$$Q_x = Q_{out} - Q_i \tag{3}$$

That is

$$Q_x = [\Delta T + (0.094)W] - [(V - 1.54) * I] \tag{4}$$

During the 50 days of the L-H operation, the rise in the electrolyte temperature during the H-periods was always higher than that calculated for Joule heating.

The present method gave rise to an estimate of the "average" input and output power (4) to within ±5% . During the 50 days that the cell was run on L-H current mode, an average excess power of approximately 18 watts (i.e., 28.8 Watts/cc of Pd) was observed during the H-periods (Fig. l.), but no excess power was observed during the L-periods. This amounts to 39 MJ of excess energy. The total input energy during the experiment amounts to approximately 230 MJ (approx. 17 %), which is based on 26.5V input for H-periods and 3.6V input for L-periods.

The degree of deuterium loading into palladium, or the d/Pd ratio, was continuously monitored during the experiment and reached 0.83 after 15 hours, remaining almost constant thereafter.

The potential of the palladium cathode was measured to determine the overpotential value. The value of the cathode potential was -1.4 V vs. S.C.E. at low current (0.25 A). The pH of the solution being 13.5, the reversible potential was calculated as -0.81 V. The resistance of the electrolyte was very nearly 1 Ω, so that the IR drop would contribute 0.25 V. This meant that the overpotential was about -0.34 V. At high current mode operation (4.2A), the potential read -5.93 V versus S.C.E. and the overpotential value was estimated as -0.92 V.

The tritium activity generated during the experiment was counted periodically, as described earlier. The activity rose to about 3 times above the background and remained constant.

III.2. RF Stimulation

After the palladium had been sufficiently loaded with deuterium, RF power was applied to the cell, maintaining the d.c. The temperature of the cell started rising within 10 minutes of the application of RF. The rate of increase in temperature was proportional to the power of the RF. After the RF signal was turned off, the electrolyte returned to room temperature within 10 minutes.

Two other frequencies, viz., 533.688 MHz and 81.924 MHz were also found to trigger exothermic effects in deuterated palladium. The heating effect only occurred during the stated frequencies and disappeared at other

frequencies. Also, such a heating effect was not observed in a H_2O system.

The experiment was carried out in an open cell configuration. The cell was not thermostated. The ambient laboratory temperature, however, was constant to within ±0.5° C. The excess power is shown in Fig. 2 as a function of frequency. Heating of the cell by RF alone did not seem to occur as the following experience demonstrates:

When 1 Watt of amplified RF at 81.924 MHz was applied to the cell, the temperature increased initially then decreased slowly over a period of 120 minutes finally reaching room temperature. During this period, the RF power remained constant. One Watt of RF power alone is expected to increase the temperature of 15 ml electrolyte by about 5°C. If RF power alone had caused the temperature change, the temperature should have increased and then remained constant rather than slowly decreasing.

There were two other observations during this experiment:

1) Just before the manifestation of the exothermic effect, the cell voltage began to fluctuate. The steady applied voltage of 3.6V fluctuated between 2.65 and 4.10 V for about 1 to 3 minutes and then settled down at 3.6 V.

2) During the fluctuations, the cell temperature initially decreased by 0.5 to 1.5°C before starting to rise [such observations have been made earlier (l&5)].

III. 3. Magnetic Stimulation

After the cathode had been charged with deuterium for 48 hours at a current of 80 mA, the cell was placed in the field of a permanent magnet with 200 Gauss strength. 230 seconds after the placement, the cell electrolyte temperature rose to 5°C (Fig. 3.). After 576 seconds, the magnet was replaced by two one-inch Neodymium magnets with a 800 Gauss field. It was placed as decribed earlier. The temperature immediately started increasing and reached 13.5°C in about 15 minutes and remained constant. The temperature returned to 3.5°C when the magnet was removed.

III.4. Materials Science

The microscopic investigations revealed some characteristic morphological changes that were brought about in Palladium by electrolysis. The investigations took place across different experimental conditions including electrolysis for six weeks, at overpotentials up to -1.0 V. Throughout all these studies, no changes were observed on the electrode surface by SEM. These changes decreased exponentially with depth (Fig. 4.) and were difficult to observe at a depth below 1 μm. The changes were manifest on the subsurface, that was obtained after etching. The observations began at a depth of 2,000 Å. Regular patterns which resembled hexagons (Fig. 5. a.) appeared. Similar hexagons have been mentioned by Brooks et al (6). Microvoids, in the form of black spots of 2,500 Å dimensions, were seen along the sides of these hexagons. There was a progression in the formation of the hexagons and the microvoids with variations in overpotential, time and temperature.

III. 4.1. Effect of H_2O in place of D_2O

Examination of sub-surface changes obtained by electrolyzing both in KOH and KOD suggests that the frequency of microvoid formation at η = - 0.35, is 3 to 5 times greater in D_2O than in H_2O. However, at η = - 0.50 V, the frequency of microvoid formation in H_2O seems about the same as in D_2O.

III. 4.2. Effect of overpotential

To study the effect of overpotential on sub-surface structural changes, electrodes were subjected to

different overpotentials at 20°C for 0.5 hours. At overpotentials more positive than -0.20 V, the sub-surface remained unaffected.

The first "visible" changes, detected by means of SEM at a magnification of 1000 (i.e., microvoids were >1000 Å), were observed at overpotential of - 0.35 V. At η more negative than - 0.35 V, the hexagon patterns, mentioned above, could be observed. The sides were approximately 3 μm in length. However, such patterns were visible only on 2 - 3 % of the total sub-surface and were scattered.

Black spots or microvoids were found at the nodes of the "hexagons," i.e., at the intersection of grain boundaries (Fig. 5.a.). There were up to 6 microvoids per hexagon cell. With an increase of overpotential to η = - 0.50 V, the changes on the sub-surface extended to ~ 5 % of the total surface and the microvoids per hexagon increased in number, from 6 at - 0.35 V to 30 at - 0.50 V (Fig. 5.b.). At more negative overpotentials, η = -l.00 V, ruptures appeared on the sub-surface of the electrode (Fig. 5.c.).

Intensive and extensive ruptures appeared on the sub-surface. The intensive ruptures were ~ 20 μm in size and covered approximately 7 % of the surface. Extensive ruptures were 5 to 10 μm in size and were distributed over ~ 20 % of the sub-surface. These ruptures were grouped into patches, each having the dimensions of ~ 0.5 mm.

III. 4.3. Effect of time

The effects observed on the palladium electrode upon electrolysis for various periods of time are shown in Figs. 6. a - d. In order to evaluate the effect of time, over the range of 0.5 hour to six weeks, an η of -0.35 V was maintained at a constant temperature of 20 °C.

For the shortest period studied, t = 0.5 hours (Fig. 6.a.), hexagons were scattered over 2 to 3 % of the total surface. As the time was prolonged to 3 hours, the hexagons increased and tended to group together to form "islands" (Fig. 6.b.). Each island contained between 20 and 50 unit hexagons. The hexagons spread to 10 % of the electrode area at 3 hours (Fig. 6.b.) and 20 % at 10 hours (Fig. 6.c.). Here, islands were formed. Each had between 200 and 300 hexagon units, were separated by about 20 to 25 μm, and tended to "cluster" into groups. The clusters had dimensions of the order of 500 μm and were seen about 1 mm apart. Fig. 6.d shows the situation after 100 hours of electrolysis.

When the Palladium electrodes were subjected to electrolysis for 6 weeks (1000 hours) the whole sub-surface was "damaged" and the hexagonal units could no longer be seen.

III.4.4. Effect of temperature

Experiments were conducted at -0.35 V for 0.5 hour at 20 and 5O°C (Fig. 7. a. and b.**).** Island formation at 50°C resembled the behavior at η = -1.0 V at 0.5 hours.

IV. DISCUSSION

IV.1. Electrochemical Stimulation

The electrochemical stimulation experiment, performed in a manner similar to that of Takahashi, showed an unmistakable generation of excess energy. As Takahashi had observed, excess heat was manifest within two days after High-Low current pulsing mode was started. There are, however, some observations that differ from those reported by Takahashi:

1. The cell voltage during the L-periods remained constant at 3.6V. The temperature of the electrolyte during these periods was close to 20°C in this experiment, suggesting no excess energy. The current during the L-periods was 0.25 A, which meant that the current density was O.O2 A. cm^{-2}. Earlier observations (7 to 10) have indicated that this current density is too low to manifest excess heat. Takahashi (2), however, reports "significant temperature increases even for L-periods."

2. There was excess energy of approximately 18W during the H-periods throughout this experiment. This is lower than what is quoted by Takahashi. It is to be mentioned here that though Takahashi first reported a relative excess of ~ 70% (3), excess was much lower (~30%) when he repeated the experiment (4).

3. Though there was a constant excess energy during the H-periods, there was no "surface boiling" that was reported in (2); again, this effect was absent in the subsequent experiment (4).

4. The degree of loading of deuterium into the cathode was continuously monitored and its value was 0.83. Takahashi did not measure but assumed it to be ~ 0.9. The overpotential was -*0.92* V.

IV.2. Pulsing and its Mechanism

It has been pointed out by Gittus and Bockris (11) that the solubility of H in Pd is greater than that of D. Also, solubility is particularly high at dislocations, because of the relation between C_σ and local stress (equation 5).

$$C_\sigma = C_o e^{\frac{\sigma V_H}{RT}} \tag{5}$$

It follows that reactions, which may be the origin of the heat production phenomenon, are likely to occur at high concentration points near dislocations within the crystal (12).

Now, there is always some H in the solution and in an unannealed electrode; thus, H may block dislocation positions from being occupied by D. Hence, pulsing, during which the D/Pd is varied up and down, may be seen as dissolving some of the H from its blocking positions on the dislocations - leaving them open to be filled increasingly with D.

This suggests that deep anodic pulsing to bring D/Pd towards zero followed by rapid cathodic pulsing to bring it up again [cf. (l)], would be the most likely switch-on mechanism.

IV.2. Radio-Frequency Stimulation

The Deuterium nucleus in the Pd-D is partly ionic and partly covalent (13). Particularly when the D/Pd ratio is greater than 0.8, effectively neutral D atoms in the lattice can 'sense' the presence of the orbital electron. This results in the generation of a fine structure magnetic field at the deuterium nucleus (14).

Calculation of Fine Structure Magnetic Field

The fine structure magnetic field is the field generated at the deuterium nucleus by the orbital motion of the electron. It was calculated from the following equation (15):

$$H = Q / R^2 * Vel / C \tag{6}$$

where

H = Magnetic field in Gauss
Q = Electronic charge ($4.802 \chi 10^{-10}$ stat.coulomb)
R = Bohr radius (5.3×10^{-9} cm) Vel = Orbital velocity of the electron ($2.2 \times l0^8$ cm/Sec)
C = velocity of light (2.997×10^{10} cm/Sec)

The magnetic field was calculated as 1.2535 x 10^5 Gauss or 12.535 Tesla.

Calculation of the frequency of stimulation

The frequency, *v*, is required to resonate and induce spin transitions in a neutron, proton or a deuterium nucleus (NMR Frequency) in a magnetic field of H. It is given by the equation (16):

$$v = \mu * \beta * H / h * I \tag{7}$$

where

v = frequency in Hz
μ = magnetic moment (0.8574 β for deuterium, 2.7927 β for proton and 1.9132 β for neutron)
β = Nuclear Magneton (5.05×10^{-24} Erg/Gauss)
H = magnetic field (1.2535×10^5 Gauss)
h = Planck's constant (6.625×10^{-27} Erg. Sec.)
I = Spin Number, 1 for Deuterium and 0.5 for proton and neutron

v was calculated as 81.924 MHz for deuterium, 365.608 MHz for neutron and 533.688 MHz for proton.

Thus, the exothermic effect observed at these specific frequencies may be related to spin orientations, occuring within the deuterium nucleus in the PdD lattice. It is not clear at the moment how and why these spin orientations cause excess heat.

It is interesting that the excess heat, caused by RF stimulation, reaches a maximum value and, after a certain time, falls to zero. A possible explanation is that the RF stimulates only the deuterium nucleus at the near surface of Pd. It is well known that, due to the 'skin effect,' high frequency alternating currents are felt only up to a certain depth (called 'skin depth') which is given by (17):

$$d = 1/(\pi * f * \sigma * \mu)^{1/2} (metres) \tag{8}$$

where,

d = skin depth
σ = electrical conductivity of the material (mho/metre)
μ = permeability of the material (Henry/metre)
f = frequency of the a.c. (Hz)

For the frequencies that have been applied in this stimulation experiment, the depth to which the RF would have been effective is only ~ 0.007 mm (7μm) .

Summary of Observations

1) RF energy at three specific frequencies triggers exothermic effect in deuterated palladium without the presence of an external magnetic field.
2) A similar effect is manifest in the presence of a magnetic field of 200 Gauss or greater.
3) The triggering is effective even at electrolysis current densities below 100 mA/cm^2.
4) Sufficient deuterium charging of the palladium (D/Pd probably greater than 0.8) is a necessary prerequisite to the triggering effect.

IV.3. Materials Science

IV. 3.1. Initiation of subsurface damage with respect to overpotential and pressure

A well-known pressure theory is useful in the discussion of the switch-on potential for cracking (18) . The D evolved on the electrode surface is assumed to be in equilibrium with D_2 in voids. If the pressure (~ fugacity) in the voids exceeds the spreading pressure, the crack will spread and damage will be detectable.

In this study, damage was found to begin at an overpotential of -0.35 V (Fig.8.). In addition, the Tafel line measurements show a sharp increase in slope in this region. The sharp increase may correspond to the saturation of the electrode surface. It may also correspond to a change of mechanism, from one in which the coupled discharge:

$$M+D_2O+e \xrightarrow{R.D.S.} M-D+OD^- \qquad (9)$$

$$M-D+M-D \rightarrow 2M+D_2 \qquad (10)$$

changes to fast discharge slow chemical combination.

$$M+D_2O+e \rightleftharpoons M-D+OD^- \qquad (11)$$

$$M-D+M-D \xrightarrow{R.D.S.} 2M+D_2 \qquad (12)$$

In the latter case, the fugacity of D_2 is given by:

$$f_{D_2} = e^{\frac{-2\eta F}{RT}} \qquad (13)$$

The condition for the beginning chemical combination of damage can then be shown to be

$$e^{\frac{-2\eta F}{RT}} \geq \left(\frac{16}{3}\frac{\gamma Y}{1}\right)^{\frac{1}{2}} \qquad (14)$$

and

$$\eta_{crit} = \frac{RT}{2F}\ln\left(\frac{16}{3}\frac{\gamma Y}{1}\right)^{\frac{1}{2}} \qquad (15)$$

where

γ = surface tension of Pd = $1.5.10^3$ dynes.cm.$^{-2}$
Y = Young's Modulus = $0.45.10^{12}$ dynes .cm^{-2}
1 = the length of the initial crack, assumed to be lens-like = 10^{-5} cm

Therefore, η_{crit} = -0.30 V , which is in excellent agreement with the observed value needed to begin cracking.

IV.3.2. Effect of overpotential

If both the extensive and intensive ruptures are taken into consideration, the percent of change on the

electrode surface has an exponential behavior. By plotting the log of the percent of change of the electrode surface as a function of overpotential (Fig.9), a linear relationship with the slope of 295 mV/decade is obtained. Thus, for the surface to change by one order of magnitude, it is necessary to increase potential by ~300 mV. This is in agreement with the previously observed change in Tafel slope from ~150 to 350 mV/decade upon reaching the overpotentials of η > - 0.35 V.

IV.3.3. Effect of time

In Fig. 10, the percent of change on the electrode subsurface is shown as a function of time of electrolysis. Two linear relationships are shown: one for the time period of 0.5 to 10 hours, and one from 10 to 1000 hours of electrolysis. The largest subsurface changes occur during the first ten hours of electrolysis.

IV.3.4. Hexagon formation

Hexagons appear as a result of plastic deformation and slip. The disappearance of hexagons at higher overpotentials is a consequence of increased loading and, hence, fracture (19,20).

IV.3.5. Time to reach saturation of the first 10/μm layer

There is much evidence in Cold Fusion Phenomena (21) which suggests that essential phenomena occur within the first 10μm of the surface. Therefore, one has to calculate the time for saturation at that depth.

The two main shapes of electrodes used are rectangular and cylindrical. For a planar surface, the concentration $C_{x,t}$, is given by:

$$C_{x,t} = \frac{2C_0 x}{\sqrt{\pi D t}} e^{\frac{-x^2}{4Dt}} \qquad (16)$$

or

$$\frac{C_{x,t}}{C_0} = \frac{2x}{\sqrt{\pi D t}} e^{\frac{-x^2}{4Dt}} \qquad (17)$$

where

C_0 = initial surface concentration
x = distance from the surface
t = time

This equation can be solved for different t at $x = 10^{-3}$ cm., when D= 10^{-7}, 10^{-8} and 10^{-9} cm^2 sec.$^{-1}$(22).

Correspondingly, for a cylindrical electrode, the concentration can be given by:

$$C = C_o - \frac{2C_o}{2.4048} \frac{J_o(2.4048\frac{r}{R})}{J_1(2.4048)} e^{-\frac{(2.4048)^2}{R^2}Dt} \qquad (18)$$

where J_0 and J_1 are the roots of Bessel's differential equation.

The concentration profiles for different times of electrolysis, calculated for both types of electrodes, are shown in Fig. 11. a. and b. In reality, the switch-on times are generally longer than the times shown here.

IV.3.6. Electronic state of dissolved hydrogen

Pure palladium is paramagnetic. A number of experimental studies (23) indicate that upon absorption of hydrogen, there is decrease in paramagnetism. In addition, the results of different authors (23) agree that when the value of H/Pd is 0.65, the solids become diamagnetic. Thus, after a D/Pd ratio of 0.65, electrons are not filling the d-band of the host metal and magnetic susceptibility is zero. As a result, electrons become more localized with respect to protons. After reaching the D/Pd ratio of 0.80, all octahedral places in the lattice are occupied and those in tetrahedral positions are now available. Consequently, hydrogen becomes much less mobile. It can be speculated that a covalent bond between Pd and H is starting to form.

Wipf (24) has compiled some experimental data on the effective charge number of hydrogen isotopes in polycrystalline Pd (Table 1).

IV.3.7. Charge on Deuterium

There are two methods of determining the charge on D^+. One method is to measure the diffusion coefficient and then (e.g., with tritium marking) obtain the mobility. Then, using the Nernst-Einstein Equation, one can find the charge, Z. Another method to determine Z is from the magnetic susceptibility.

There is a linear decrease of magnetic susceptibility to D/Pd = 0.65 after which the d holes are filled and the susceptibility tends to zero.

The value of Z is clearly near to 0.5 at low values of D/Pd (Fig. 12.), and decreases as D/Pd increases. At D/Pd =0.8, the likely value of Z from magnetic susceptibility measurements is decreasing to zero.

IV.4. Theories of Cold Fusion

IV.4.1. Difficulties in Cold Fusion as seen by classical Nuclear Physicists

Difficulties in Cold Fusion, as seen by classical nuclear physicists, are as follows:

1) Penetrating the coulomb barrier
2) That nuclear and chemical processes take place at radically different frequencies (e.g., 10^{14} sec^{-1} and 10^{22} sec^{-1}) (This is referred to as "asymptotic freedom" by Preparata (25).)
3) The Leggett-Baym (26) point, which is that deuterium ions in the palladium lattice are further apart than they are in the deuterium molecule. Therefore, as the authors saw it, the ions must remain stably apart.

As to the columb barrier penetration, it is invalid to apply a simple Gamow formula to calculate the tunneling probability in metals, as is done in the dilute plasma. Thus, in the metal the approach to collision is through an electron gas which screens the charges from each other and thus reduces the barrier. A Gamow calculation is inapplicable.

The insulation of the nucleus from chemical forces seems incompatible with the fact that Mossbauer frequencies depend upon the chemical surrounds of the nucleus.

The Leggett-Baym point is a difficulty. Even in the tetrahedral positions, the D-D distances are 1.77 Å -- too large.

However, if the Gittus- Bockris hypothesis is pursued, i.e., the activity is at dislocations, the solubility is greatly enhanced and D/Pd in those areas must be » 1. If it is >3, the tetrahedral holes are filled when the D/Pd at the dislocations exceeds 3, the only possibilities are interstitial positions when the D-D distances are are smaller.

3.4.2. Anomalous phenomena which act as criteria for the correctness of models

The essential phenomena of Cold Fusion- small rate of production of neutrons, large rate of production of tritium, heat more than between 10 and 100 (occasionally 1,000) watts per cc of Pd- are well known.

However, a successful theory must be consistent with the following:

1. The sporadicity of observation of the effects,
2. Switch-on is dependent upon impurities in the solution, or the metal,
3. Switch-on does not occur for times of the order of 100 hours of electrolysis.

3.4.3. Types of Theories

1. The fusion of D + D in the bulk of a metal lattice [Preparata(25); Takahashi(27)] .
2. The fusion of D + D at promontories on the surface of the electrode [Bockris(28); Kim(29)].
3. Production of tritium and heat with a mechanism which involves "virtual" neutrons [Hagelstein(30)].
4. Transmutational reactions [Kucherov(31)].

IV.4.3.1 Fusion in the bulk

IV.4.3.1.a. Preparata Model (25)

The most comprehensive attempt to give a credible theory of this is due to Preparata(25) with an application of his ideas of super radiance (particles behave in a coherent fashion within the lattice).

This theory does take notice of the electronic structure of transition metals. The model of a metal tacitly assumed by most workers is that of a series of individual (non-bonded) cations interspersed by essentially free electrons. But transition metals are bonded (32) and share electron orbits in a three dimensional manner. Preparata utilizes the properties of the d electron level in palladium to make a rudimentary theory of such screening, and deduces therefrom a reduction in the equivalent barrier height(Jones Fusion). At this point, to increase the rate of fusion to attain the observed heat, Preparata introduces his hypothesis that there are groups of electrons (400 Å) and groups of deuterons (1,000 Å) which move coherently.

Such a model would give rise to extreme heating in the hot spot regions of the coherent groups and therefore destroy their structure which, in this model, is the origin of the enhanced fusion. For this reason, Preparata brings in "electron cooling." He shows that the excess heat is "taken away" by the coherent electron groups.

Preparata's theory has the virtue of leaning upon the real electronic structure of palladium. However, after having got to the Jones limit quite rationally, it needs faith, i.e., that the coherent groups which he assumes, must be assumed to exist. Further, it gives no interpretation of the facts brought out above as those most characteristic of cold fusion experiments, their sporadicity; their dependence upon specific surface structures and the abnormally long time they take to switch on (longer than that to reach D/Pd = 0.83 near the surface).

IV.4.3.2. Surface Promontory Models

The first of these was proposed in 1990 by Bockris et al.(28) on the basis that observations made of successful electrodes showed that their surfaces possessed a dendritic structure.

On this basis, a model was suggested which depended upon the high field developed at tips of low radius of curvature [Bockris and Gonzales-Martin(33)].

Thus, the evolution of deuterium preferentially occurs at these tips and and they become associated sporadically with bubble formation. When these bubbles attain a certain size, the high field at the tip of the dendrites then emits electrons into the deuterium in the gas containing the bubble and ionizes some of the D_2. ($D_2 + e \rightarrow D^+ + D$).

A zeroeth approximation theory was given by Packham, et al (34), still assuming a D^+ ------- D^+ relation and a Gamow barrier. But since that time, it has been realized that the dendrite tips have ADSORBED D, which may have a zero or even a negative charge. This model does not have a Coulomb barrier.

The theory at first seemed to be a hot fusion theory, hence consistent only with n/T=l. However, in the cluster impact work (35), there is the same high reaction rate for the tritium-proton channel and a low rate for the conventional He^3 + neutron level, as is observed in cold fusion. It is found here that the pre-exponential factor of the Gamow equation is 10^{25} times larger for the low energies involved here rather than for the high ones in classical nuclear physics.

This suggestion of a preferred channel for tritium solves the principal difficulty suffered by the original dendrite theory of Bockris et al (28).

The dendrite theory has advantages over competing theories because it explains the factors which are anomalous in other models. Thus, it depends upon the surface conditions, because only some surfaces will grow dendrites. The dendrites may not consist only of palladium, they may be of other materials grown from the solution. Furthermore, the growth of dendrites would depend upon the impurities in solution, in a characteristic way as developed by Popov (36). Briefly, the rate of growth would depend exponentially upon the impurities in the solution. Irreproducibility obtains an interpretation, as do long switch-on times.

Thus, the dendrite theory not only explains the anomalous n/T ratios formation but it also gives a quantitative interpretation of the surface sensitivity, the dependence upon impurities, and the long time for delay. Such features are not possessed by any other theory.

IV.4.3.3. Theory involving Neutron Transfer

This theory is due to P. L. Hagelstein (3O) and has a principal point as its foundation: the Coulomb barrier is difficult to overcome without some special mechanism such as the high field arising at points of minimal curvature, so that it is clear that a mechanism which avoids it is welcome.

In Hagelstein's view, this can be achieved by assuming that neutrons from deuterons transfer to "acceptor" nuclei such as another deuteron, ^6Li, ^{10}B or to Pd itself, entering their nuclei to produce various products including tritium (cf. Kucherov's model).

On the other hand, Hagelstein, by avoiding the coulomb barrier, involves a difficulty, namely, the distance the neutrons would have to travel to achieve the reaction which he suggests. Thus, only "virtual" neutrons are available to him and it is easy to calculate the life time of such a particle.

Hagelstein's model is of great interest because it would appear to give a step towards the production of various new nuclei as observed by Kucherov. The major problem is to lengthen the life time of "virtual" neutrons by, say, 10^5 times.

IV.4.3.4 Transmutational Theories

Karabut, Kucherov and Sawatimova (31) have suggested a theory based upon experiments that they have carried out in glow discharge experiments in the presence of deuterium. They observe characteristics which are similar to those which are observed in aqueous solution, excess heat, weak neutron generation, tritium and He^4 production, together with characteristic X-rays and weak gamma radiation.

The novel feature of their work is that they analyze their cathodes chemically, finding, of course, helium and tritium similar to the findings earlier published by Bockris et al. However, they utilize an X-ray microprobe, high resolution dipole mass spectrometry and secondary high mass spectrometry and find a host of new elements in the palladium as a result of the electrolysis. Thus, they found not only ^6Li, but also several other metals from groups one and two and then also Ca, Cr, Ni, Ge, etc. These elements occur in the upper 1 micron layer of the cathode, in consistency with the concept of the surface reaction as the origin of fusion. The content of the transmuted elements is up to 0.1 atomic %.

Karabut et al. observed that the presence of germanium is wholly unexpected. The maximum concentration is 0.1 atomic %.

The possible reactions suggested by Karabut et al. are given in Fig. 13.

Very approximate calculations which have been made by Karabut et al. seem to suggest that the right order of magnitude of heat can be obtained on the basis of these suggested reactions.

ACKNOWLEDGMENTS

Financial support from ENECO (formerly FEAT) is acknowledged. Z.M. thanks the Welch Foundation for a partial support for this work. R.S. thanks the Bhabha Atomic Research Centre, Bombay (India) for leave of absence.

VI. REFERENCES

1. J. O'M. Bockris, D. Hodko and Z. Minevski, ICCF-2, June-29 -July 4, 1991, Como, Italy, p.337.
2. A. Takahashi, et al., Int. J. Appl. Electromagn. Materials, 106,1(1992).
3. J. O'M. Bockris, et al, ICCF-4, December 6-9, 1993, Maui, USA.
4. A. Takahashi, et al., ICCF-3, Oct. 21-25, 1992, Nagoya, Japan,p. 79.
5. M. Fleischmann, S. Pons and M.Hawkins, J. Electroanal.Chem., 261, 301(1989).
6. C. R. Brooks and A. Choudhury, Metallurgical Failure Analysis, McGraw-Hill, Inc., 1993, p.182.
7. S. Pons and M. Fleischmann, Proc. 1st Annual Conference on Cold Fusion, March 28-31, 1990, Salt Lake City, Utah(USA), p.l.
8. M. C. H. McKubre, et al, "Frontiers of Cold Fusion" (Proc. 3rd International Conference on Cold Fusion, Oct.21-25, 1992, Nagoya, Japan), Universal Academy Press, Japan, p.5.
9. E. Storms, Ibid., p.21.
10. K. Kunimatsu, et al, Ibid., p.31
11. J. Gittus and J. O'M. Bockris, Nature, 339 (1989) 105.
12. J. O'M. Bockris and P. K. Subramanyan, ActaMetall., 19 (1971) 1205.
13. J. Knaak and W.Eichenauer, Z.Naturforsch.,239(1968)1783.
14. A.W. Overhauser; Physical Review, 92(1953)411.
15. K. R. Atkins; "Physics", 2nd Edition, John Wiley, New York,1970,p.303.
16. CRC Handbook of Chemistry and Physics, 66th Edition, 1985-1986, CRC Press, Boca Raton. (Florida), 1985, Table E-75.
17. D. W. Dearholt and W. R. McSpadden; "Electromagnetic Wave Propagation", McGraw-Hill, 1973, p.174.
18. J. O'M. Bockris and A. K. N. Reddy, Modern Electrochemistry, Plenum, New York, 1970.
19. C. R. Brooks and A. Chaudhury, "Metallurgical Failure Analysis", McGraw-Hill, 1993, p.185.
20. H.Bohm In "An Atlas of Metal Damage", L. Engel and H. Clingele (Ed), Carl Hanser Verlag, Munich, Germany,1981.
21. C. C. Chien, D. Hodko, Z. Minevski and J. O'M. Bockris, J. Electroanal. Chem., 338 (1992) 189.
22. S. Majorowski and Baranowski, J. Phys. Chem. Solids, 43 (1982) 1119
23. F. A. Lewis, “The Palladium System,” Academic Press, London (1967), p.147.
24. H. Wipf, "Hydrogen in Metals", Vol. II, G. Alefeld and J. Volkl (Ed.), Springer-Verlag, Berlin, (1978), p.273.
25. G. Preparata, Fusion Technology, 20 (1991) 82.
26. A. J. Leggett and G. Baym, Nature, 340 (1989) 45.
27. A. Takahashi, et al, Preprint of the paper submitted to the Russian Conference 011 Cold Fusion, Abrau-Durso, Russia,Sept.1993.
28. G. H. Lin, R. C. Kainthla, N. J. C. Packham and J. O'M. Bockris, J. Electroanal. Chem., 280 (1990) 207
29. Y. E. Kim, Fusion Technology, 19 (1991) 558.
30. P. Hagelstein, ibid., 23 (1993) 353; also a preprint of the paper to be communicated to Fusion Technology.
31. A. B. Karabut, Y. R. Kucherov and I. B. Sawatimova, "Frontiers of Cold Fusion " [Proc. 3rd International Conference on Cold Fusion, Oct.21-25, 1992, Nagoya, Japan], Universal Academy Press, Tokyo, 1993, p.165.
32. L. Pauling and E.B. Wilson, Introduction to quantum mechanics, Chapter 12, McGraw -Hill, 1935.

33. A. Gonzales-Martin, R. C. Bhardwaj and J. O'M. Bockris, J. Applied Electrochemistry, 23 (1993) 531.
34. N. J. C. Packham, K. L. Wolf, J. C. Wass, R. C. Kainthla and J. O'M. Bockris, J. Electroanal. Chem., 270 (1989) 451.
35. R. J. Beuhler, G. Friedlander and L. Friedman, Phys. Rev. Lett., 63 (1989) 1292.
36. K. I. Popov and M. D. Maksimovic, in J. O'M. Bockris et al. (eds), Modern Aspects of Electrochemistry, Volume 19, p. 193. Plenum Press, N.Y. (1989)

Table 1.

HYDROGEN ISOTOPE	H/Pd or D/Pd	T (K)	EFF . CHARGE NUMBER, Z*	EXPER. TECHNIQUE
H	High (α-phase)	290-350	positive, +1 for H/Pd=O . 6	Drift velocity
H	$<2.8 \times 10^{-2}$	455-513	+0.4 to +0.55	H_2 flux meas .
H	$<1.6 \times 10^{-2}$	520-620	+0.54	H_2 flux meas .
D	$<1.0 \times 10^{-2}$	520-620	+0.51 to +0.59	H_2 flux meas .
H D	$<4.0 \times 10^{-2}$	420-1070	Between + 0.3 and +0.7	H_2 flux meas .
H, D	$<8.2 \times 10^{-3}$	970	+0.35	Diff. potent.

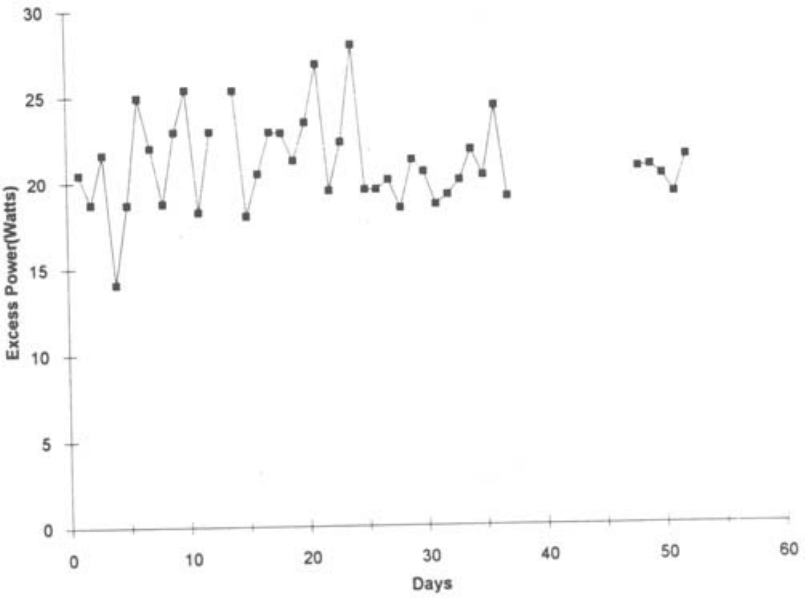
Excess Power(Watts)
30
25
20
15
10
5
0
0
10
20
30
40
50
60
Days

Fig. 1.

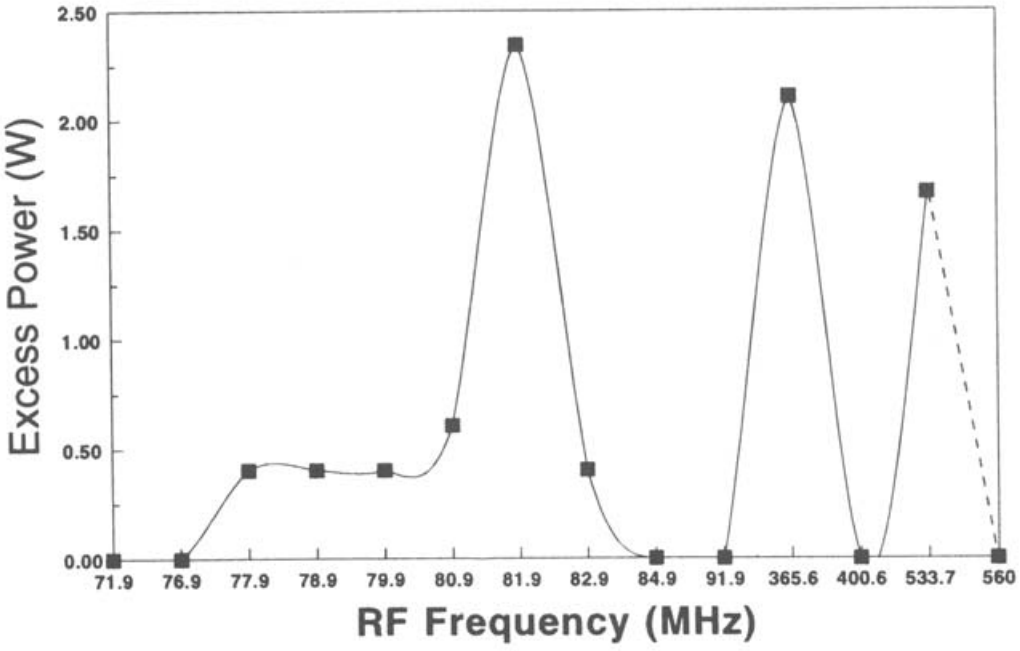
Excess Power (W)
2.50
2.00
1.50
1.00
0.50
0.00
71.9
76.9
77.9
78.9
79.9
80.9
81.9
82.9
84.9
91.9
365.6
400.6
533.7
560
RF Frequency (MHz)

Fig. 2.

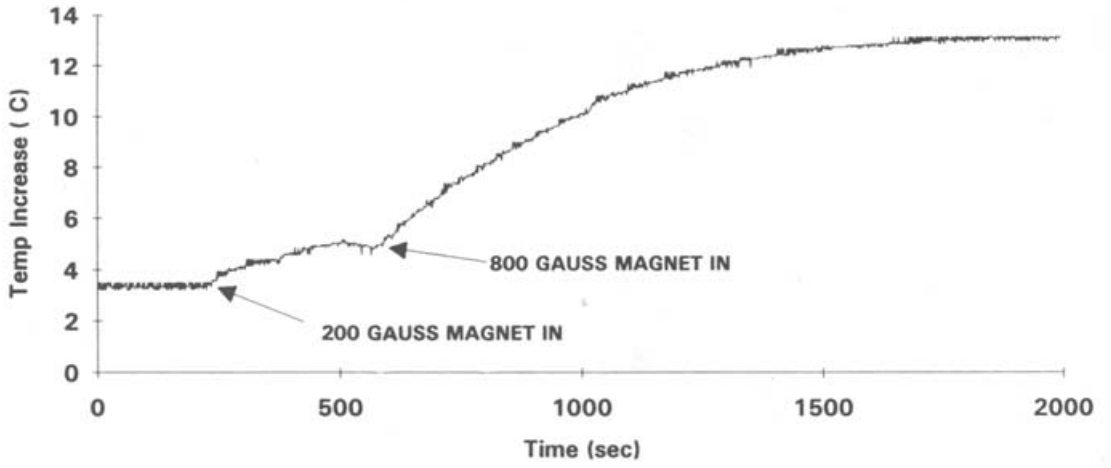
Temp Increase (C)
14
12
10
8
6
4
2
0
0
500
1000
1500
2000
Time (sec)
800 GAUSS MAGNET IN
200 GAUSS MAGNET IN

Fig. 3.

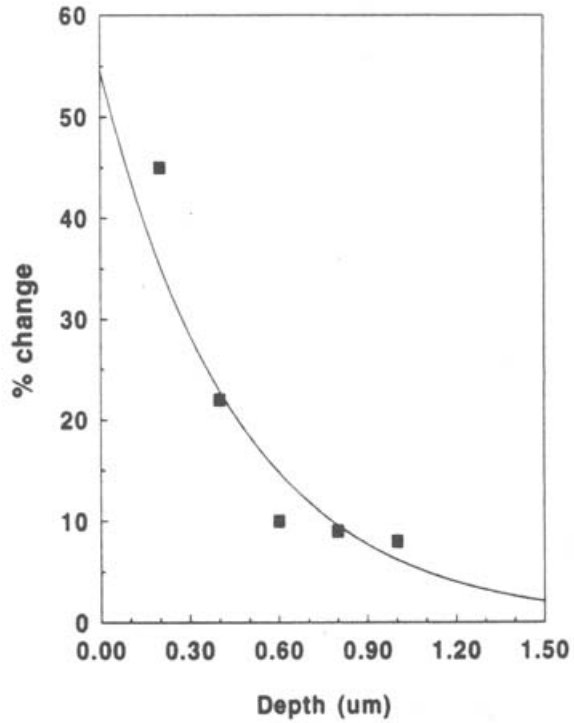
% change
60
50
40
30
20
10
0
0.00
0.30
0.60
0.90
1.20
1.50
Depth (um)

Fig. 4.

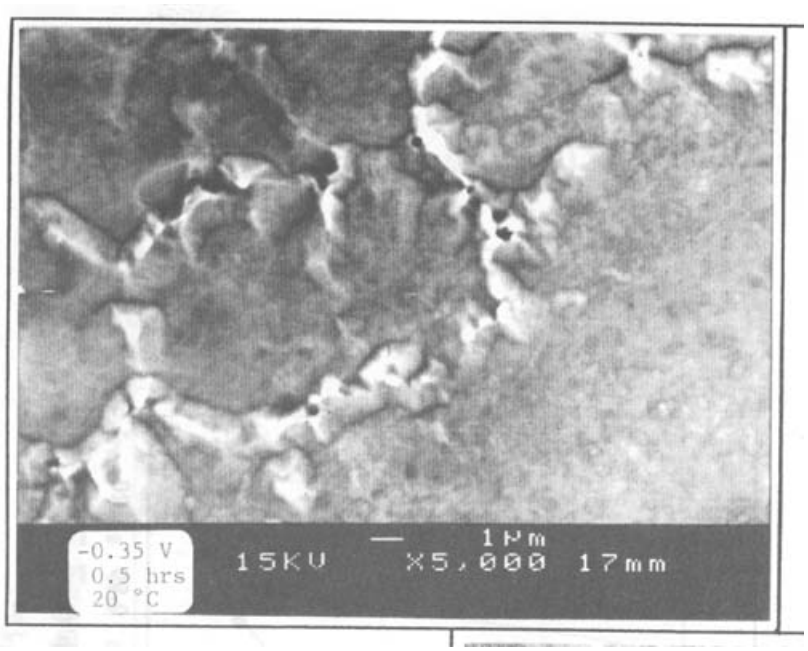
-0.35 V
0.5 hrs
20 °C
15KV
1µm
X5,000 17mm

Fig. 5. a.

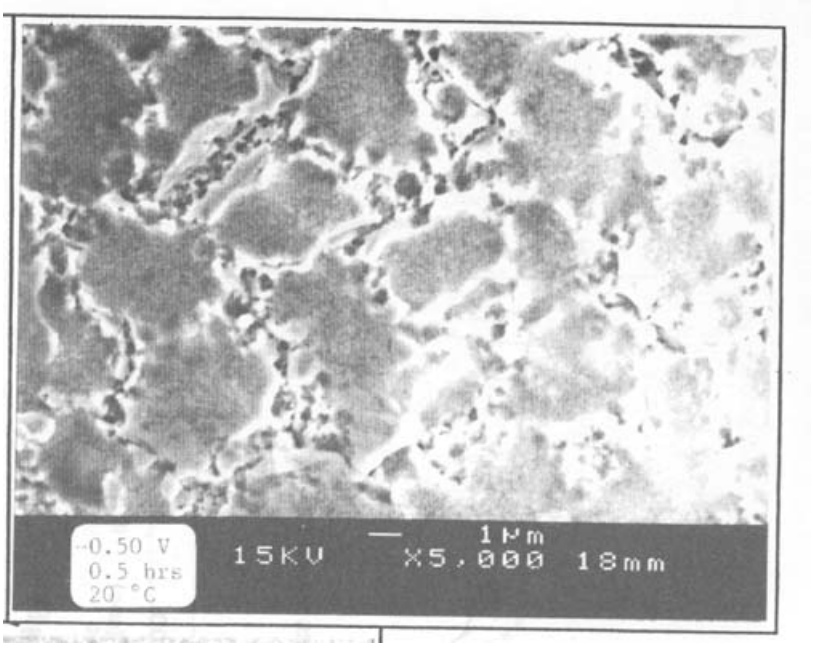
-0.50 V
0.5 hrs
20 °C
15KV
1µm
X5,000 18mm

Fig. 5. b.

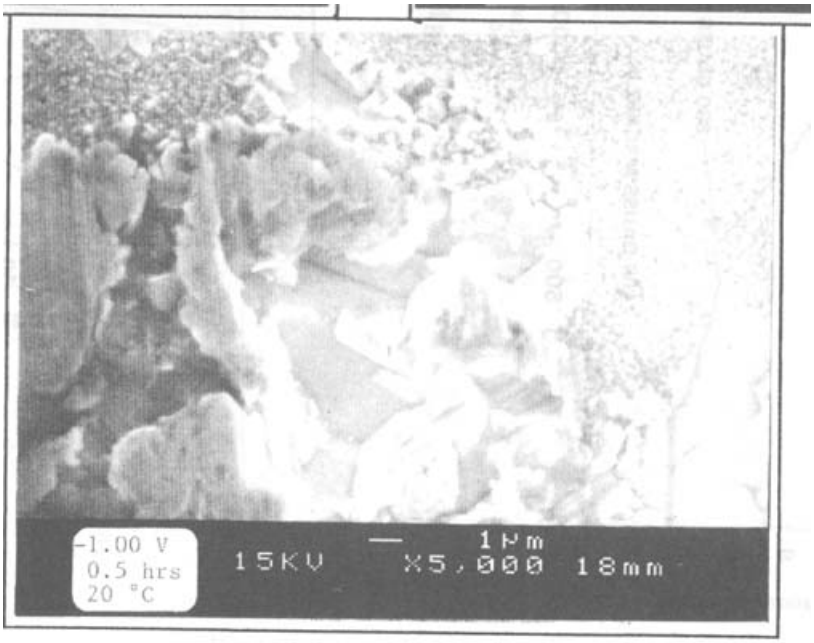

Fig. 5. c.

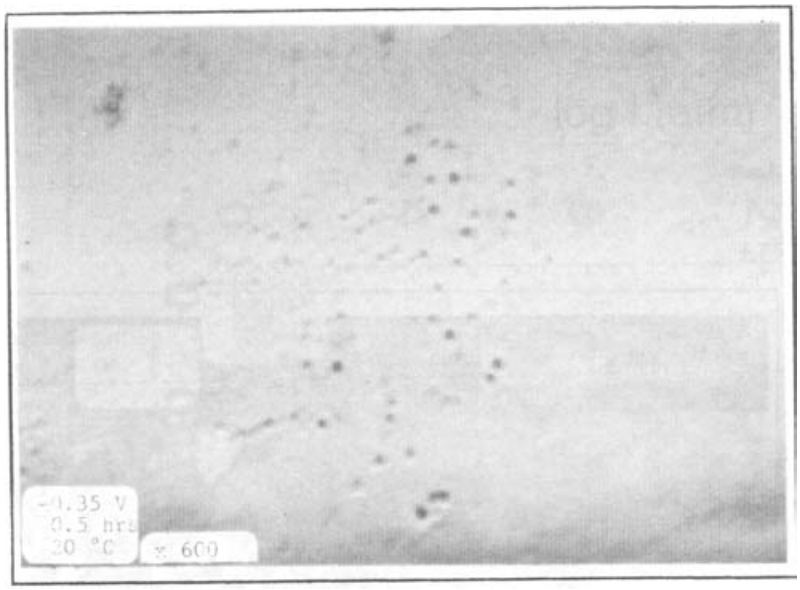

Fig. 6. a.

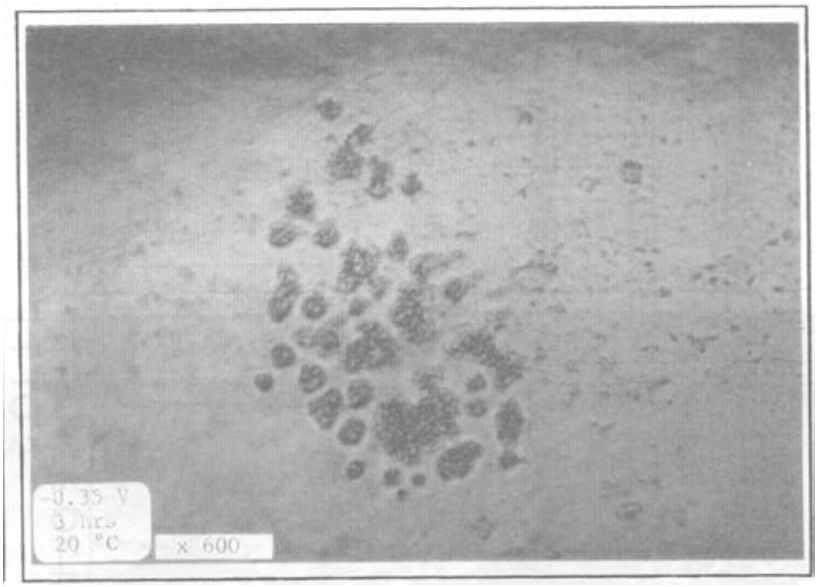

Fig. 6. b.

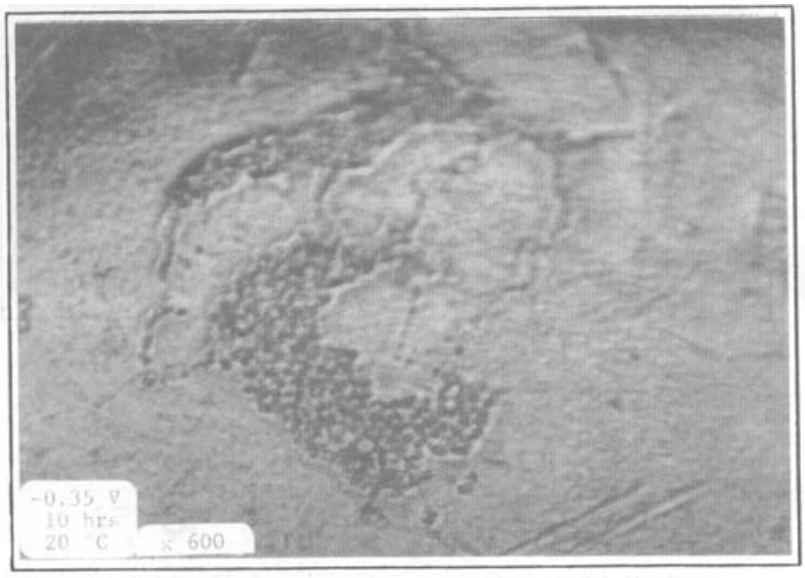

Fig. 6. c.

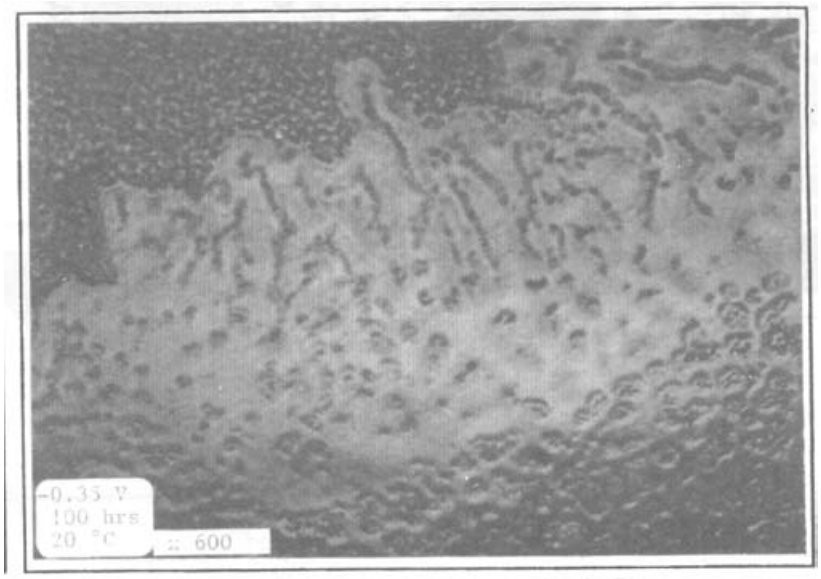

Fig. 6. d.

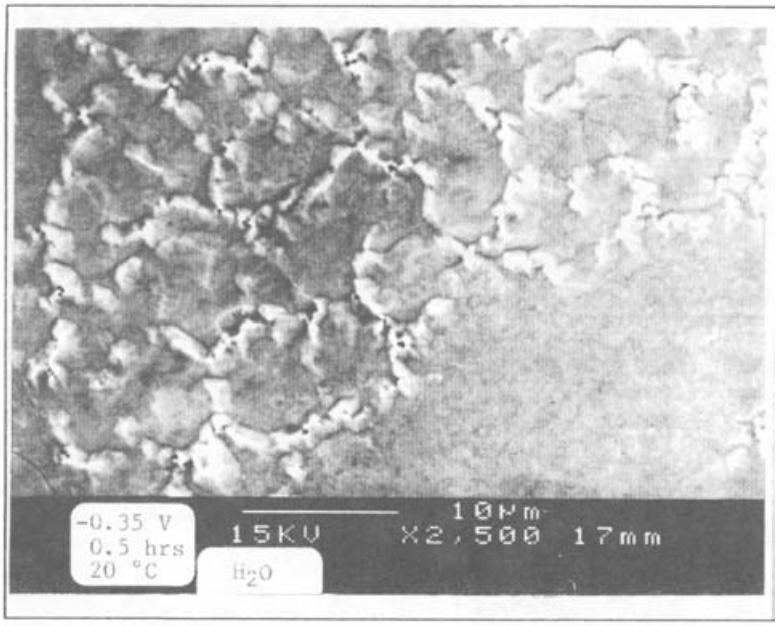
-0.35 V
0.5 hrs
20 °C
H2O
15KV
10µm
X2,500 17mm

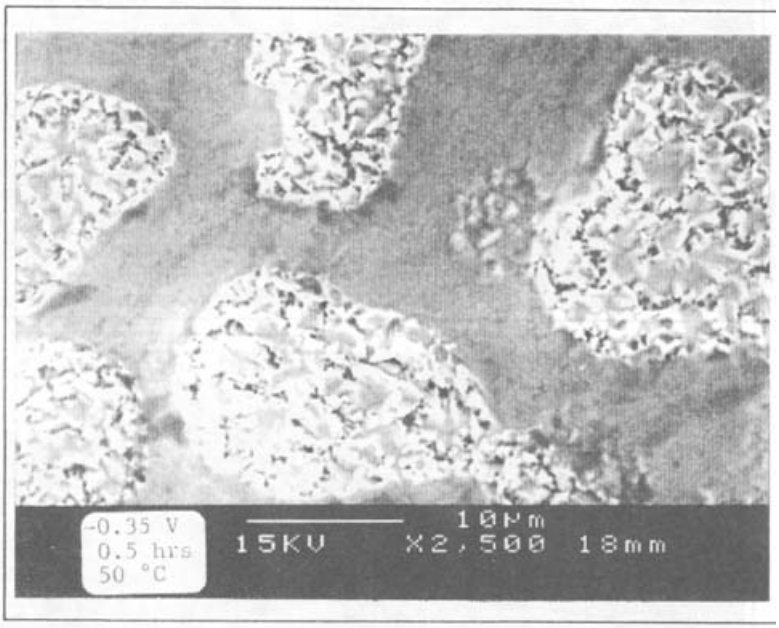
-0.35 V
0.5 hrs
50 °C
15KV
10µm
X2,500 18mm

Fig. 7. a – b.

MECHANISM 1. COUPLED DISCHARGE CHEMICAL DESORPTION

OVERPOTENTIAL < -0.35 V $$f_{D_2} = 10^{1.5} e^{-\frac{1}{2}\frac{\eta F}{RT}}$$

MECHANISM 2. FAST DISCHARGE SLOW CHEMICAL COMBINATION

OVERPOTENTIAL > -0.35 V $$f_{D_2} = e^{-\frac{2\eta F}{RT}}$$

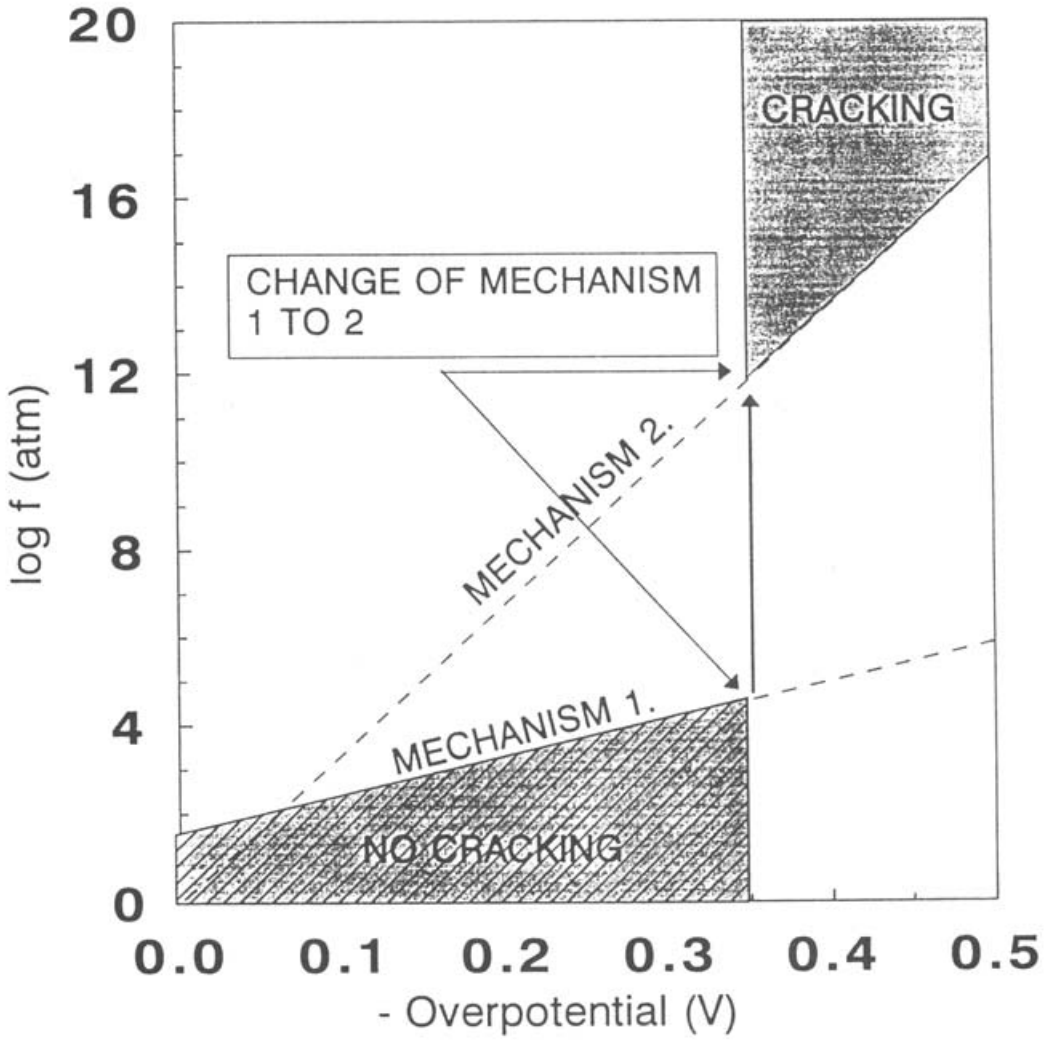

Fig. 8.

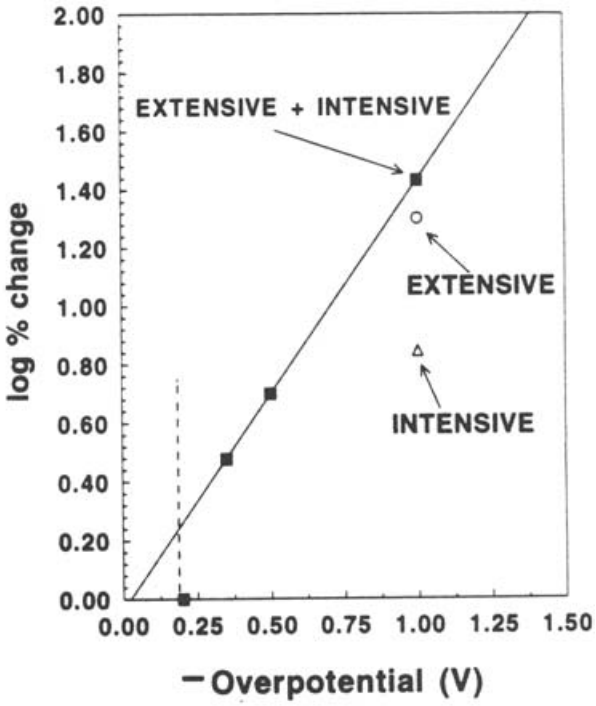
2.00
1.80
1.60
1.40
1.20
1.00
0.80
0.60
0.40
0.20
0.00
log % change
EXTENSIVE + INTENSIVE
EXTENSIVE
INTENSIVE
0.00 0.25 0.50 0.75 1.00 1.25 1.50
− Overpotential (V)

Fig. 9.

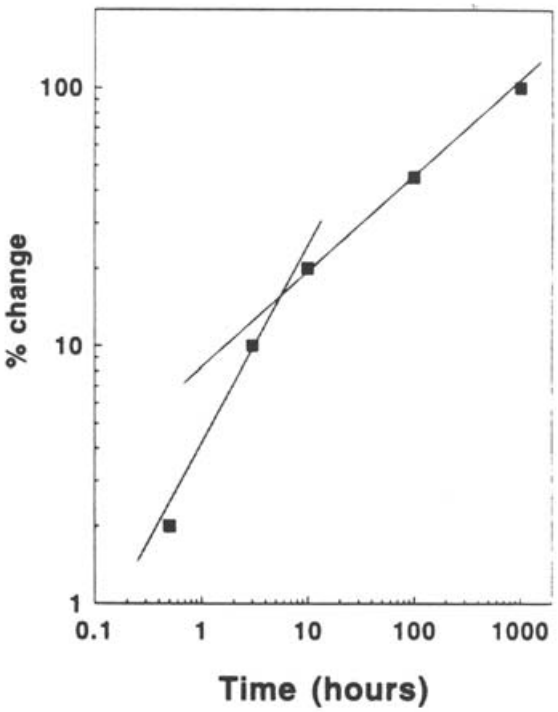
100
10
1
% change
0.1 1 10 100 1000
Time (hours)

Fig. 10

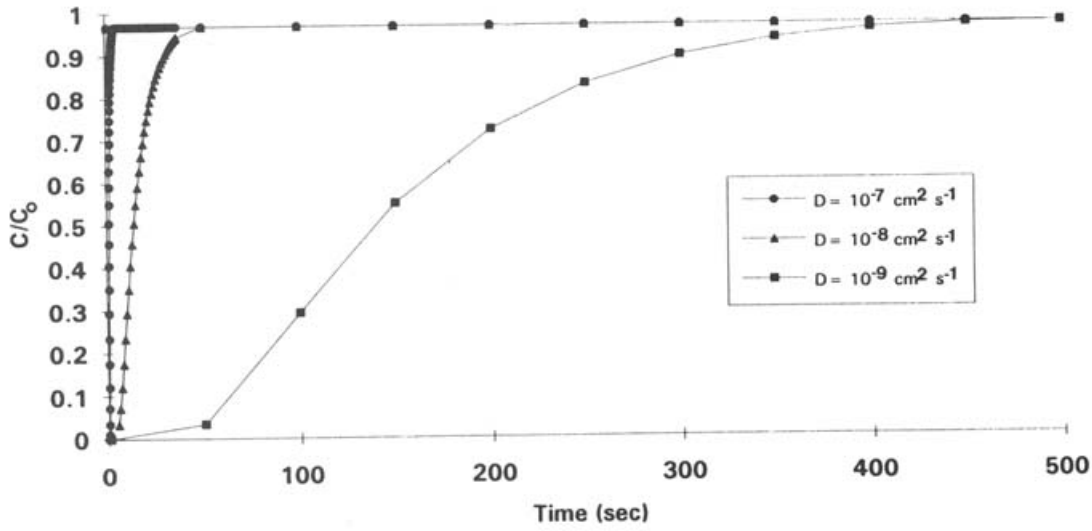

Fig. 11. a.

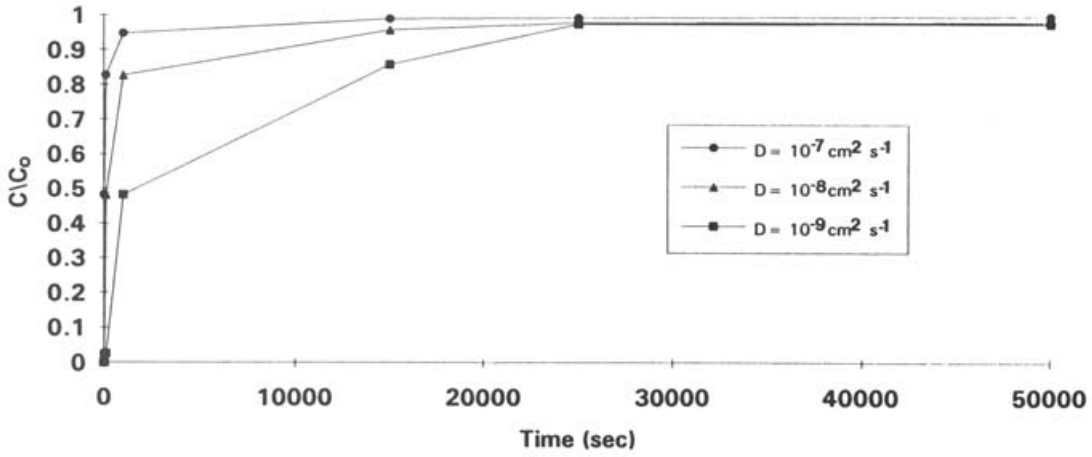

Fig. 11. b.

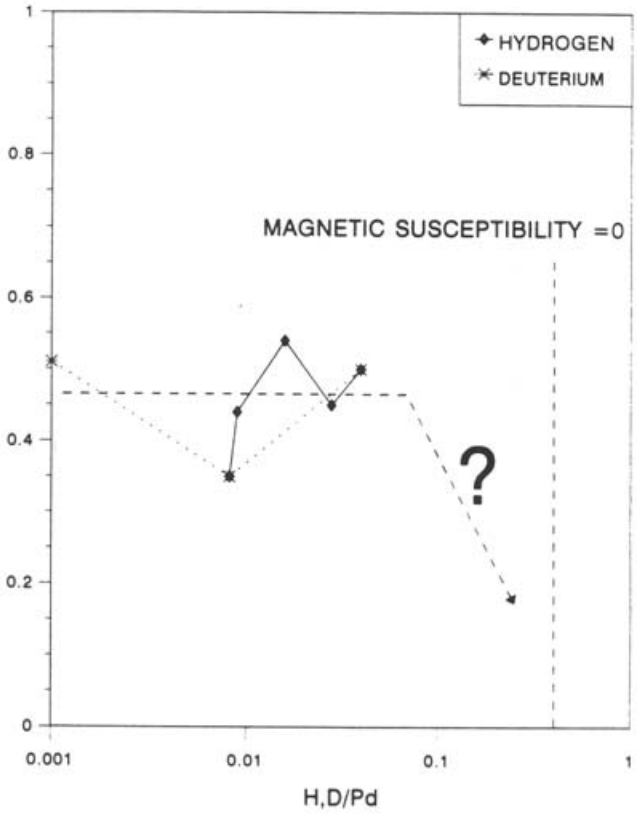
HYDROGEN
DEUTERIUM
MAGNETIC SUSCEPTIBILITY =0
?
1
0.8
0.6
0.4
0.2
0
0.001
0.01
0.1
1
H,D/Pd

Fig. 12.

KUCHEROV'S REACTION SCHEMES

$_{46}Pd \rightarrow {}_{36}Kr + {}_{10}Ne$
$\rightarrow {}_{34}Se + {}_{12}Mg$
$\rightarrow {}_{30}Zn + {}_{16}Sn$
$\rightarrow {}_{24}Cr + {}_{22}Ti$

$_{46}Pd + D \rightarrow {}_{42}Mo + {}_{5}B$
$\rightarrow {}_{40}Zr + {}_{7}N$

$_{46}Pd + 2D \rightarrow {}_{38}Sr + {}_{10}Ne$
$\rightarrow {}_{42}Mo + {}_{6}C$
$\rightarrow {}_{46}Pd^{*} + {}_{2}He$

$_{46}Pd + 3D \rightarrow {}_{44}Ru + {}_{5}B$
$\rightarrow {}_{46}Pd^{*} + {}_{3}Li$

Fig. 13.